YALE
PEABODY
MUSEUM

P.O. BOX 208118 | NEW HAVEN CT 06520-8118 USA | PEABODY.YALE. EDU

JOURNAL OF MARINE RESEARCH

The *Journal of Marine Research,* one of the oldest journals in American marine science, published important peer-reviewed original research on a broad array of topics in physical, biological, and chemical oceanography vital to the academic oceanographic community in the long and rich tradition of the Sears Foundation for Marine Research at Yale University.

An archive of all issues from 1937 to 2021 (Volume 1–79) are available through EliScholar, a digital platform for scholarly publishing provided by Yale University Library at https://elischolar.library.yale.edu/.

Requests for permission to clear rights for use of this content should be directed to the authors, their estates, or other representatives. The *Journal of Marine Research* has no contact information beyond the affiliations listed in the published articles. We ask that you provide attribution to the *Journal of Marine Research*.

Yale University provides access to these materials for educational and research purposes only. Copyright or other proprietary rights to content contained in this document may be held by individuals or entities other than, or in addition to, Yale University. You are solely responsible for determining the ownership of the copyright, and for obtaining permission for your intended use. Yale University makes no warranty that your distribution, reproduction, or other use of these materials will not infringe the rights of third parties.

This work is licensed under a Creative Commons Attribution-NonCommercial-ShareAlike 4.0 International License.
https://creativecommons.org/licenses/by-nc-sa/4.0/

Journal of Marine Research, 68, 433–457, 2010

Relative displacement probability distribution functions from balloons and drifters

by J. H. LaCasce[1]

ABSTRACT

The focus of relative (pair) dispersion studies in the atmosphere and ocean is often on the mean square particle separation or the Finite Scale Lyapunov Exponent. Much less attention has been paid to the probability density function (PDF) of pair separations, despite that this determines the dispersion. In two-dimensional (2-D), nondivergent, homogeneous flows, the PDF is governed by a Fokker-Planck equation. Analytical solutions exist for the turbulent inertial ranges, but these have rarely been compared to observations.

We consider the analytical PDFs for the turbulent inertial ranges and derive a new solution for the 2-D energy range. We then compare the analytical PDFs with those generated with data from three *in situ* sets: one from a balloon experiment in the stratosphere and two from surface drifter experiments in the ocean. For comparison, we also consider PDFs from a numerical simulation of 2-D turbulence forced at intermediate scales. The results suggest that dispersion at sub-deformation scales is nonlocal, with pair separations growing exponentially in time. This implies the kinetic energy spectra at these scales are at least as steep as κ^{-3}. The dispersion at larger scales is harder to characterize because of the uncertainty in the PDF at larger separations, but the results are consistent with previous inferences. In general the PDF provides useful information on the spreading which can be difficult to discern from the dispersion alone.

1. Introduction

Relative dispersion concerns how pairs of particles, initially near one another, separate in time. It is relevant for the spreading of passive and active tracers, for example spilled oil in the ocean and volcanic ash in the troposphere. While the displacement of a tracer cloud is determined by the mean velocity of the particles in the cloud, the spreading about its center of mass is determined by the relative motion of pairs of particles. Relative dispersion is also of theoretical interest because pairs simultaneously measure fluid velocities at separate points in space. In homogeneous flows, the mean square difference between the particles' velocities is equivalent to the second order Eulerian structure function, and the latter is related to the kinetic energy spectrum. Thus relative dispersion can be used to make inferences about the spectral slopes, with certain limitations (Bennett, 1984; Babiano *et al.*, 1990).

1. Department of Geosciences, University of Oslo, P.O. Box 1022 Blindern, 0315 Oslo, Norway. ***email: j.h.lacasce@geo.uio.no***

Relative dispersion has been examined in observational studies in both the atmosphere and ocean (Morel and Larcheveque, 1974; Er-el and Peskin, 1981; Davis, 1985; LaCasce and Bower, 2000; LaCasce and Ohlmann, 2003; Ollitrault *et al.*, 2005; Koszalka *et al.*, 2009; Lumpkin and Ellipot, 2010). Recent reviews are given by LaCasce (2008a) and Salazar and Collins (2009). Many of these studies suggest the dispersion differs qualitatively above and below the deformation radius. At the largest separations, where the pair motion is generally uncorrelated, the dispersion reflects the general circulation. Thus large-scale dispersion in the lower stratosphere is zonally anisotropic (Morel and Larcheveque, 1974), due to the zonal shear. In the North Atlantic it is more nearly isotropic (LaCasce and Bower, 2000; Ollitrault *et al.*, 2005), as dispersion is steered by topography (LaCasce, 2000).

On the other hand, several studies indicate consistent behavior below the deformation radius, where pair velocities are generally correlated. Studying balloons in the Southern Hemisphere stratosphere, Morel and Larcheveque (1974) and Er-el and Peskin (1981) found that pair separations grew exponentially in time (in the EOLE and TWERLE experiments, respectively). Similarly, LaCasce and Ohlmann (2003) observed exponential growth at sub-deformation scales at the surface in the Gulf of Mexico, Ollitrault *et al.* (2005) observed the same in the eastern North Atlantic and Koszalka *et al.* (2009) found exponential growth in the Nordic Seas.

For a two-dimensional, homogeneous flow, exponential growth occurs when the energy spectrum is "nonlocal," or steeper than κ^{-3} (Bennett, 1984; Babiano *et al.*, 1990). So the aforementioned results imply the energy spectra at sub-deformation scales are at least as steep as κ^{-3}. Exponential dispersion could reflect 2-D turbulence, as the spectrum under a 2-D enstrophy cascade has a κ^{-3} dependence (Kraichnan, 1967; Charney, 1971). But the spectra could also be steeper. Shepherd *et al.* (2000) suggest this is the case in the stratosphere, so that the paradigm of *chaotic advection* is relevant. Chaos implies a sensitive dependence on initial conditions, and the exponential dispersion reflects a sensitivity to the particle's starting position.

But whether exponential growth occurs at all scales below the deformation radius is unclear. Lacorata *et al.* (2004) re-examined the EOLE balloon data using a different measure (the Finite Scale Lyapunov Exponent or FSLE). While they found exponential growth at scales below 100 km, the results for the range from 100 km up to the deformation radius, approximately 1000 km, were more consistent with Richardson's Law, in which the mean square pair separation increases as time to the third power (Richardson, 1926). This would imply an energy spectrum with a $\kappa^{-5/3}$ slope, as found in a turbulent energy cascade (Kraichnan, 1967; Sec. 2). Similarly Lumpkin and Ellipot (2010), who used the FSLE with surface drifter pairs from the western North Atlantic, maintained that Richardson dispersion was occurring below the deformation radius there as well.

The distinction is important because the slope of the energy spectrum affects how we parametrize the sub-deformation scales in numerical models. In the upper troposphere, we have independent observations of the Eulerian energy spectra with which we can compare (Nastrom and Gage, 1985). But the spectra in the ocean are not yet conclusive

(e.g., Stammer, 1997; LeTraon *et al.*, 2008; Wang *et al.*, 2010). So any information which can be gleaned from pair dispersion is of interest.

Knowing the spectra also affects how we conceptualize the dynamics at those scales. A 2-D turbulence paradigm (Charney, 1971; Salmon, 1980) would likely involve an enstrophy cascade below the deformation radius, as noted. But others have suggested that surface quasi-geostrophic (SQG) dynamics are relevant near the ocean surface and near the tropopause (Tulloch and Smith, 2006, 2009; LaCasce and Mahadevan, 2006; Lapeyre and Klein, 2006; Capet *et al.*, 2008; Isern-Fontanet *et al.*, 2008). QG and SQG turbulence have distinct characteristics,[2] so it is worth knowing which one is relevant.

However, relative dispersion by itself isn't always conclusive. As seen in the examples considered hereafter (e.g., Figs. 2, 5), it is often possible to fit *both* an exponential and a power law to the data, within the errors. So one often cannot distinguish the behavior based on relative dispersion alone.

Is it possible to do so using other measures? A number of authors suggest that the FSLE is more effective in this regard (Artale *et al.*, 1997; Aurell *et al.*, 1997; Boffetta and Sokolov, 2002; Lacorata *et al.*, 2004; Lumpkin and Ellipot, 2010). This is because the FSLE, which derives from distance-based averages rather than time-based ones, may be superior at distinguishing the spreading occurring at different spatial scales. However the FSLE often differs from relative dispersion, for reasons that remain to be fully elucidated.

Relative dispersion is the second moment of the pair separations and derives from the probability density function (PDF) of the separations. As is well known, the second moment may not be a good statistical indicator if the PDFs are strongly non-Gaussian. Previous observations (Er-el and Peskin, 1981; Davis, 1985; LaCasce and Bower, 2000; LaCasce and Ohlmann, 2003; Koszalka *et al.*, 2009) suggest the separation PDFs are indeed non-Gaussian, at least at sub-deformation scales. If so, we must consider higher order moments, or look at the PDFs themselves.

Hereafter we do the latter, using data from various observations. These include the EOLE balloons and the surface drifters studied by LaCasce and Ohlmann (2003) and Koszalka *et al.* (2009). We compare the separation PDFs with analytical solutions of a Fokker-Planck equation, under different turbulence cascade scenarios, and to PDFs obtained with a turbulence simulation. The results yield a fairly consistent indication of the dispersion occurring at small scales.

2. Theory

Motivated by observations of spreading smoke plumes, Richardson (1926) proposed a Fokker-Planck (F-P) equation governing the pair separation PDF under turbulent dispersion. Kraichnan (1966) derived a similar equation using his Lagrangian Direct Interaction

2. SQG turbulence possesses two inertial ranges, an inverse cascade for total energy with a κ^{-1} slope and a direct cascade for temperature variance, with a $\kappa^{-5/3}$ slope (Held *et al.*, 1995).

Approximation and Lundgren (1981) showed that the same could be obtained with a velocity field delta-correlated in time; see Bennett (2006) for an overview. For a homogeneous, incompressible 2-D flow, the equation is:

$$\frac{\partial}{\partial t}\, p = \frac{1}{r}\frac{\partial}{\partial r}\left(\kappa_2\, r \frac{\partial}{\partial r}\, p\right) \tag{1}$$

where r is the pair separation, $p(r, t)$ is the PDF and:

$$\kappa_2 = \frac{1}{2}\frac{d}{dt}\langle r^2 \rangle \tag{2}$$

is the relative (longitudinal) diffusivity. The brackets indicate the average over all available pairs and the factor of 1/2 is traditional. The equation can be solved via the Laplace transform or by an appropriate change of variables, with specified initial conditions.

A familiar example is when the pair velocities are uncorrelated. Then the relative diffusivity is constant (and equal to twice the single particle diffusivity, e.g., Babiano *et al.*, 1990). In this case, the Laplace transformed F-P equation has the homogeneous solution:

$$\hat{p} = A I_0\left(\sqrt{\frac{s}{\kappa_2}}r\right) + B K_0\left(\sqrt{\frac{s}{\kappa_2}}r\right) \tag{3}$$

where I_0 and K_0 are modified Bessel functions of order zero. We assume a delta-function initial condition:

$$p(r, 0) = \frac{1}{2\pi r}\delta(r - r_0). \tag{4}$$

The pre-factor insures that the probability is normalized, i.e. that:

$$2\pi \int_0^\infty p\, r\, dr = 1. \tag{5}$$

Note that here, and in the subsequent cases, we assume the dispersion is isotropic. Taking the inverse transform of the particular solution yields:

$$p(r, t) = \frac{1}{4\pi\kappa_2 t}\, \exp\left(-\frac{r_0^2 + r^2}{4\kappa_2 t}\right)\, I_0\left(\frac{r_0 r}{2\kappa_2 t}\right). \tag{6}$$

In the long time asymptotic limit, in which $r \gg r_0$ and $\kappa_2 t \gg r$, this reduces to:

$$p(r, t) = \frac{1}{4\pi\kappa_2 t}\, \exp\left(-\frac{r^2}{4\kappa_2 t}\right). \tag{7}$$

which is proportional to the Rayleigh distribution.

Using the asymptotic distribution, we can derive the raw moments:[3]

$$\langle r^n \rangle = 2\pi \int_0^\infty r^{n+1}\, p\, dr = (4\kappa_2 t)^{n/2}\, \Gamma\left(\frac{n}{2}+1\right), \tag{8}$$

where Γ is the gamma function. Thus the second moment, the relative dispersion,

$$\langle r^2 \rangle = 4\kappa_2 t, \tag{9}$$

increases linearly in time, as expected for a diffusive process (Taylor, 1921). The kurtosis, the normalized fourth order moment, is given by:

$$Ku = \frac{\langle r^4 \rangle}{(\langle r^2 \rangle)^2} = 2. \tag{10}$$

This is constant, reflecting that the Rayleigh distribution is self-similar (it retains its shape).

Then there are the solutions to (1) for the turbulent inertial ranges. Richardson (1926) obtained a solution to the one dimensional analogue of (1) assuming:

$$\kappa_2 = \beta r^{4/3}, \tag{11}$$

which he deduced from observations. This pertains to the energy cascade, for which the energy spectrum is proportional to $\kappa^{-5/3}$ (Batchelor, 1950); then β is proportional to the third root of the energy dissipation rate. The same scaling applies for the inverse energy cascade in two dimensions, because the spectrum has the same slope.

Richardson's (1926) is an asymptotic solution, like the Rayleigh solution with a constant diffusivity. The full solution for a delta-function initial distribution can again be obtained via the Laplace transform. This is:

$$p(r,t) = \frac{3}{4\pi\beta t\, r_0^{2/3} r^{2/3}} \exp\left(-\frac{9\left(r_0^{2/3}+r^{2/3}\right)}{4\beta t}\right)\, I_2\left(\frac{9 r_0^{1/3} r^{1/3}}{2\beta t}\right) \tag{12}$$

The corresponding result in 3-D is given by Bennett (2006). In the long time limit ($r \gg r_0$ and $\beta t \gg r^{2/3}$), this reduces to:

$$p(r,t) = \left(\frac{3}{2}\right)^5 \frac{1}{4\pi(\beta t)^3} \exp\left(-\frac{9r^{2/3}}{4\beta t}\right). \tag{13}$$

which is the 2-D analogue to that obtained by Richardson (1926).

Using the asymptotic distribution, it is straightforward to show that:

$$\langle r^n \rangle = \frac{1}{2}\left(\frac{4\beta t}{9}\right)^{3n/2} \Gamma\left(\frac{3n+6}{2}\right). \tag{14}$$

3. We prefer raw moments to those with the means removed as separations are positive definite.

Thus the second moment is:

$$\langle r^2 \rangle = 5.2675\,\beta^3\,t^3. \tag{15}$$

The dispersion increases as time cubed, a signature of Richardson dispersion. Note the dispersion does not depend on the initial separation, as the expression derives from the asymptotic PDF. Note too that Eq. (15) provides a way of determining the constant β (and hence the energy dissipation rate) from data.

In addition, the kurtosis is given by:

$$Ku = 2\frac{8!}{(5!)^2} = 5.6. \tag{16}$$

Like the Rayleigh distribution, the Richardson PDF is self-similar, but the kurtosis is larger than 2, implying the PDF has a longer tail.

The other inertial range in 2-D turbulence is for the enstrophy cascade, with an energy spectrum proportional to κ^{-3}. In this case, the relative diffusivity scales as:

$$\kappa_2 = \frac{1}{2}\frac{d}{dt}\langle r^2 \rangle = \frac{r^2}{T}, \tag{17}$$

where the time scale T is proportional to the inverse cubic root of the enstrophy dissipation rate (Lin, 1972). The corresponding solution to the F-P equation is log-normal (Lundgren, 1981; Bennett, 2006):

$$p(r) = \frac{1}{4\pi(\pi t/T)^{1/2}\,r_0^2}\,\exp\left(-\frac{[\ln(r/r_0) + 2t/T]^2}{4t/T}\right) \tag{18}$$

The separation moments can be shown to be:

$$\langle r^n \rangle = r_0^n \exp\left(\frac{n(n+2)t}{T}\right) \tag{19}$$

So the dispersion,

$$\langle r^2 \rangle = r_0^2\,\exp\left(\frac{8t}{T}\right), \tag{20}$$

increases exponentially in time. Note the time scale T differs by a factor of 8 from the e-folding time for the dispersion. Often the two time scales are assumed equal, which follows from simply integrating relation (17) to obtain the dispersion; but doing so is incorrect because the RHS of (17) involves the square separation while the LHS involves its mean, two different quantities. Furthermore the kurtosis is:

$$Ku = \exp\left(\frac{8t}{T}\right). \tag{21}$$

Thus the Lundgren PDF (18) is *not* self-similar but becomes sharper in time, with an increasingly extended tail. An important point is that the same PDF applies to spectra which are steeper than κ^{-3}, as exponential growth occurs whenever the spectra are nonlocal (Bennett, 1984; Babiano *et al.*, 1990).

Separation PDFs have been examined previously in relation to the Richardson regime. Sullivan (1971) inferred PDFs from observations of dispersing dye on Lake Huron and compared the results to the asymptotic Richardson PDF and to an alternate PDF proposed by Batchelor (1952). Jullien *et al.* (1999) and Ott and Mann (2000) examined separation PDFs from particles in laboratory experiments and Boffetta and Sokolov (2002) did so for particles in simulated 3-D turbulence. While the results of Sullivan (1971) did not support the Richardson PDF, those of the other three studies did. Separation PDFs for the enstrophy range were calculated from laboratory simulations by Jullien (2003) and from numerical simulations by LaCasce (2010). The latter obtained PDFs consistent with Lundgren's distribution.

3. Results

Hereafter we examine three data sets, using the same approach. First we fit the observed relative dispersion with an exponential and a cubic function. This determines the constants β (for the Richardson PDF) and T and r_0 (for the Lundgren PDF). Then we calculate the PDFs for the data and compare them to the Richardson, Lundgren and Rayleigh PDFs, at various times.

a. EOLE

EOLE was a large balloon experiment in the Southern Hemisphere during the 1970s (Morel and Bandeen, 1973). The constant level balloons, many of which were launched in pairs or clusters, rose to the 200-mb level and were advected by the winds. The relative dispersion was first analyzed by Morel and Larcheveque (1974) and was re-visited by Lacorata *et al.* (2004) using the the FSLE. We examine a set of 426 pairs of these balloons, with a maximum initial separation of 25 km.

As noted by Morel and Larcheveque (1974), the EOLE dispersion is approximately isotropic up to separations of 1000 km. This is illustrated in Figure 1, which shows the ratio of the rms zonal to meridional pair displacements. For the first 2 days the displacements are comparable, but by day 3 the zonal displacement is much larger. Thus comparisons with the theoretical PDFs, which assume isotropic dispersion, are most appropriate during the first 2–3 days.

The relative dispersion for the EOLE set is plotted in Figure 2. Shown are two separate curves: one for "original pairs" (pairs launched together) and one for "chance pairs" (including pairs which were found together subsequently). All pairs have a maximum initial separation of 25 km. The solid curve is the exponential obtained by a least squares fit of the original pair dispersion during the first 2.5 days. The dashed curve is another exponential,

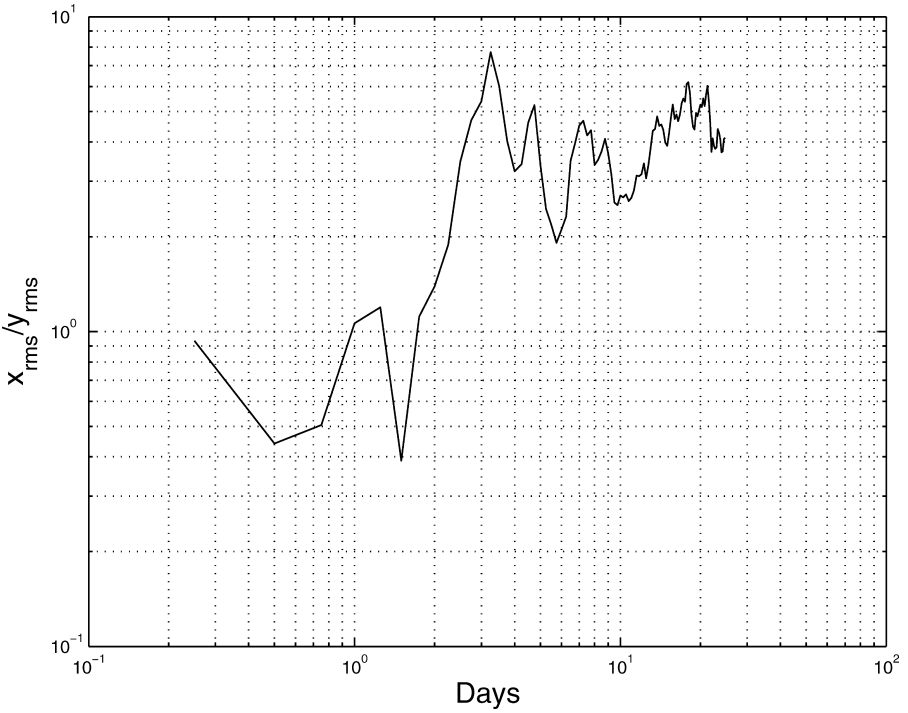

Figure 1. The rms zonal pair separation divided by the rms meridional separation for the EOLE balloons.

using the parameters of Morel and Larcheveque (1974). The dashed straight line is a cubic function and the dash-dot line is a linear one.

Fitting the original pair dispersion during the first 2.5 days yields an initial separation of 57 km and an e-folding time of 0.49 days (corresponding to $T = 3.95$ days). Fitting the chance pair dispersion on the other hand yields $r_0 = 77$ km and an e-folding time of 0.4 days ($T = 3.16$ days). Thus the e-folding times are similar, but the initial separation for the chance pairs is larger. Note too that both values of r_0 are greater than the initial spacing of the pairs, 25 km.

The initial separation for the chance pairs is close to the 80 km inferred by Morel and Larcheveque (1974). However, their e-folding time of 1.35 days is substantially larger than ours. This discrepancy evidently stems from differences in the data sets; ours is more recent and includes trajectories not analyzed by Morel and Larcheveque (1974) (A. Hertzog, pers. comm.). However, Lacorata *et al.* (2004) obtained a dispersion very similar to ours (see their Fig. 2) and an e-folding time of 0.5 days. So it is likely our data sets are similar.

After one week, the dispersion increases approximately linearly in time, consistent with Morel and Larcheveque (1974) and Lacorata *et al.* (2004). The amplitude, approximately $1.0 \times 10^6\,\mathrm{km}^2/\mathrm{day}$, is the same as that obtained by Lacorata *et al.* (2004). It is somewhat

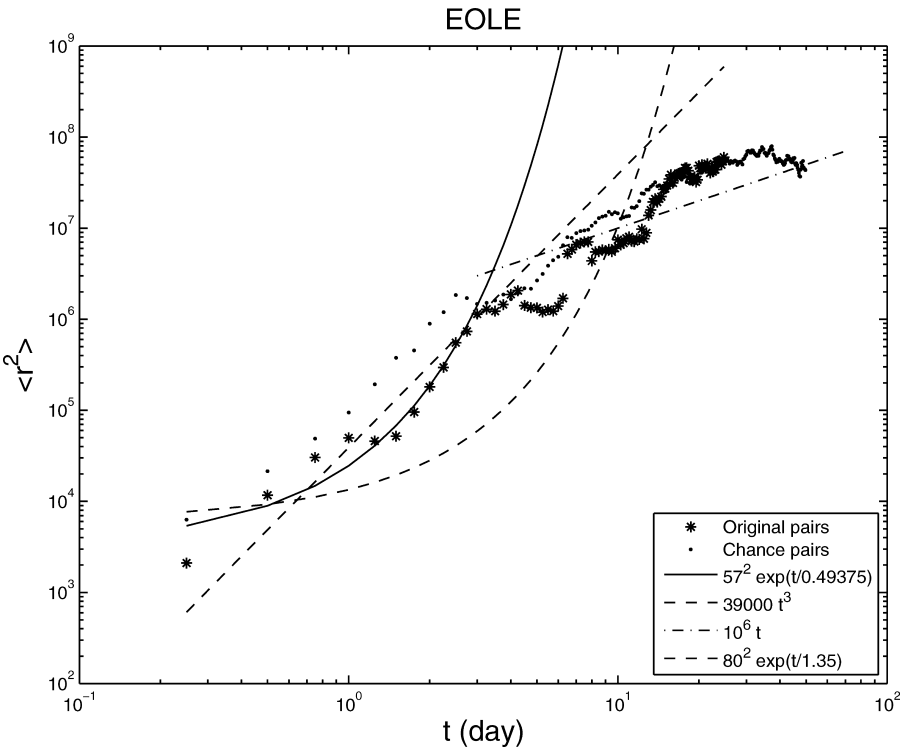

Figure 2. The relative dispersion for the EOLE balloon data. The asterisks show the dispersion for the original pairs and the dots for the chance pairs. The time spacing is 1/4 of a day. The solid curve is the exponential obtained by a least squares fit during the first 3 days for the original pairs. The dashed curve is the exponential obtained by Morel and Larcheveque (1974). The dashed line is the cubic function proposed by Lacorata *et al.* (2004). The dash-dot curve indicates linear growth.

larger than that of Morel and Larcheveque (1974) ($2.8 \times 10^5\,\mathrm{km}^2/\mathrm{day}$). However, the dispersion is noisy during this period and, moreover, is zonally anisotropic. Fitting only the meridional dispersion yields a coefficient which is ten times smaller.

One can also fit the dispersion with a cubic function. Lacorata *et al.* (2004) inferred cubic growth by examining the FSLE, and their amplitude corresponds to $\beta = 3.9 \times 10^4\,\mathrm{km}^{2/3}/\mathrm{day}$. Using that value yields the dashed line in Figure 2. This lies between the chance and original pair curves and is a plausible fit for either one. So we cannot distinguish exponential or Richardson regimes based on the relative dispersion alone.

Using the best-fit parameters for the exponential and Lacorata *et al.*'s value of β, we construct the Lundgren and Richardson PDFs. We then compare those with the PDFs for the chance pairs in Figure 3 and the original pairs in Figure 4.[4]

4. In these and the following figures, we plot for the PDFs the function $2\pi rp$. Thus the sum of this function with separation is unity.

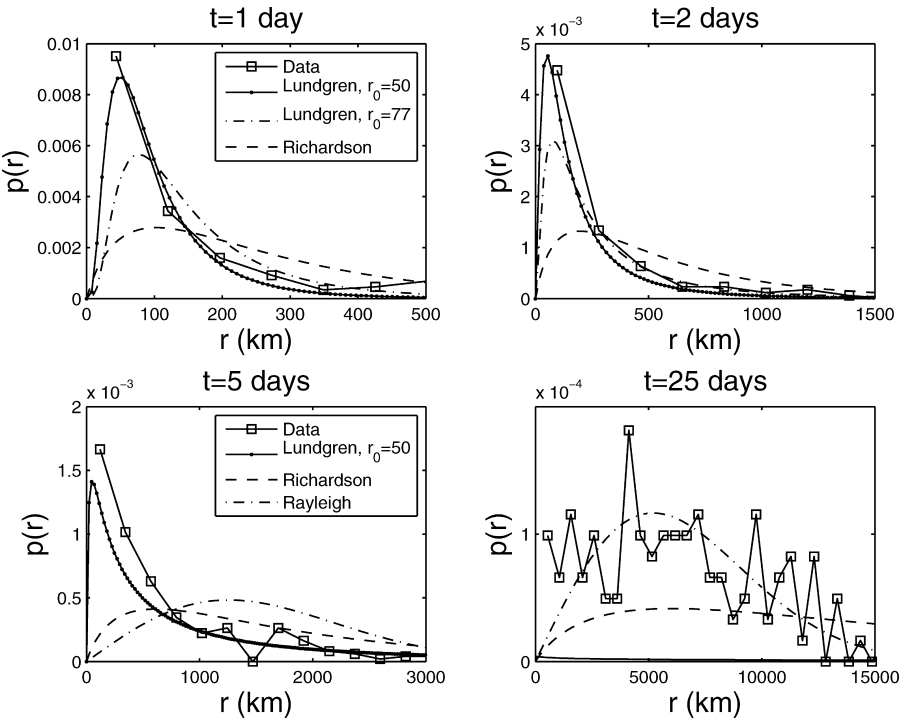

Figure 3. The separation PDFs for the EOLE chance pairs. Also shown is the Lundgren PDF from (18), with $T = 4$ days and two values of r_0 (77 and 50 km), and the Richardson PDF from (12) with $\beta = 3.9 \times 10^4$ km$^{2/3}$/day and $r_0 = 50$ km. The dash-dot curves in the bottom panels are the asymptotic Rayleigh distribution in (7) with the same variance as the data. In all cases, we plot $2\pi r p(r)$, so that the integral under the curves is unity.

Consider the chance pairs first. The observed PDFs are shown with two versions of the Lundgren PDF in the upper panels of Figure 3. The latter both have $T = 2$ days, but different values of r_0. Also shown is the full Richardson PDF from (12). At $t = 1$ day, the Richardson PDF lies well below the observed PDF. The Lundgren PDF with $r_0 = 77$ km (the best-fit value) is somewhat closer, but also lies below. But the Lundgren solution with the smaller separation, $r_0 = 50$ km, compares favorably to the data to separations of several hundred kilometers. At $t = 2$ days, the situation is the same. The Richardson PDF is still well below the observed PDF and the Lundgren PDF with $r_0 = 77$ km is closer, but the best agreement comes with the Lundgren PDF with $r_0 = 50$ km.

At $t = 5$ days, the observed PDF resembles the Lundgren PDF with $r_0 = 50$ km but also lies somewhat above it, indicating more small-scale separations. The Richardson PDF continues to lie well below. We also plot the Rayleigh PDF here, and that is substantially different than the observed. Only at $t = 25$ days does the PDF (albeit quite noisy) approach the Rayleigh.

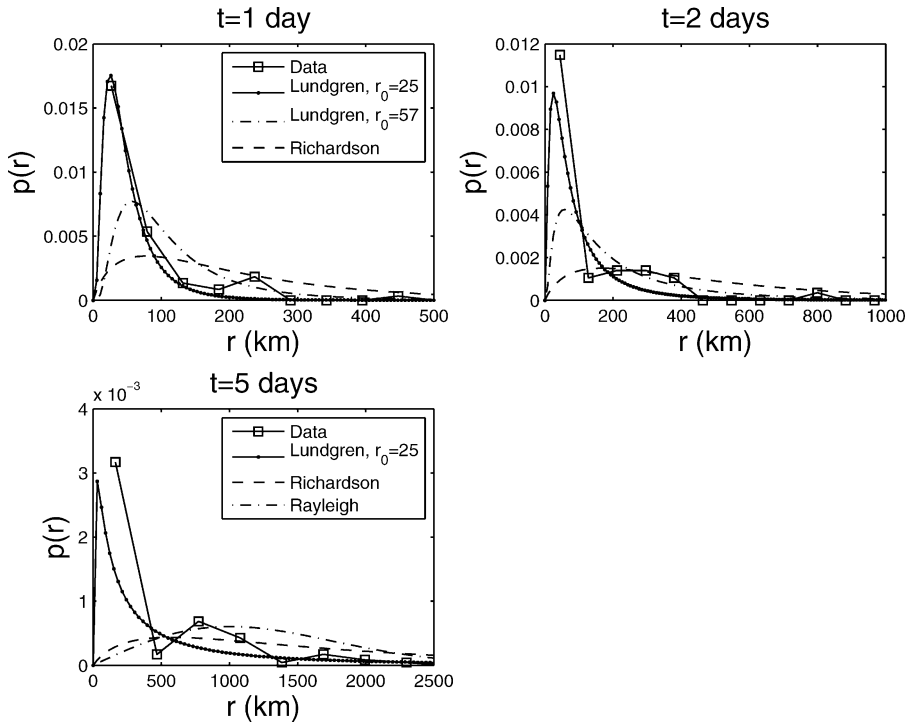

Figure 4. The separation PDFs for the EOLE original pairs, plotted with two Lundgren PDFs, with $T = 4$ days and $r_0 = 50$ km and 25 km, and the Richardson PDF with $\beta = 3.9 \times 10^4$ km$^{2/3}$/day and $r_0 = 25$ km. The Rayleigh distribution is again shown in the lowest panel.

The asymptotic Richardson PDF, given in (13) (not shown), is quite close to the full PDF, except at $t = 1$ day. Then the asymptotic PDF is closer to the Lundgren PDF with $r_0 = 77$ km, and thus still below the observed PDF. The reason is that the argument of the exponential in the asymptotic distribution goes to zero with r but does not in the full PDF; so the maximum value of the asymptotic PDF is roughly twice that of the full PDF. However, by $t = 2$ days the two curves are similar, with the maximum of the asymptotic PDF only about 40% larger than that of the full PDF. By $t = 5$ days, the difference in maxima is only about 20%. So the discrepancy with the observed PDF seen in lower left panel of Figure 3 is about the same when using the asymptotic distribution.

The PDFs for the original pairs (Fig. 4) are noisier than for the chance pairs, because there are only 184 pairs instead of 426. Nevertheless, the results are similar. The Richardson PDF lies well below the observed PDF and the Lundgren PDF with the best fit value for r_0 is only somewhat better. But the Lundgren PDF with a smaller separation, in this case $r_0 = 25$ km, is in reasonable agreement.

Thus we would infer exponential growth for both the chance and original pairs during the first 2–3 days, the period of isotropic dispersion. The PDFs for both chance and original

pairs have an e-folding time of about 0.5 days, as noted by Lacorata *et al.* (2004). However, better agreement is obtained in both cases with an initial separation *smaller* than indicated from fitting the dispersion. For the original pairs, the PDFs indicate that the correct initial separation is the maximum initial separation for the pairs, $r_0 = 25$ km.

This discrepancy in r_0 may stem from the difference in initial conditions. As noted, the theoretical curves assume a delta-function distribution while the actual PDFs are broader initially (i.e. we use all separations below 25 km). But it may also reflect a difference in how quickly pairs lose their "memory" of their initial condition, which depends on the correlation between their initial separation and velocity (Babiano *et al.*, 1990). Chance pairs, or pairs which approach one another after deployment, have such a correlation. So the adjustment to the exponential regime is plausibly extended for the chance pairs, and this would appear as a larger effective r_0 during exponential growth. Original pairs on the other hand are less likely to have correlated velocities and separations. Several authors have noted that chance pairs do not yield significantly different dispersion than original pairs (e.g. Morel and Larcheveque, 1974; Er-el and Peskin, 1981; LaCasce, 2008a; Koszalka *et al.*, 2009), but none have tested the evolving PDF. The present results suggest there is a difference—not in the growth time scale, T, but in the effective initial separation.

Another point is that the PDFs exceed the Lundgren PDF at small separations by day 5, for both sets. This occurs because the dispersion occurring at larger scales is slower than exponential, as seen in Figure 2. The Lundgren PDF presumes an exponential expansion to infinite separations and thus spreads more rapidly. So it lies farther below the observed PDF as time increases.

The PDFs suggest exponential growth early on, but over which scales is this occurring? With both sets of pairs, the agreement with the Lundgren PDF is clearest below 200 km. At larger scales, it is difficult to say whether the Richardson or Lundgren PDF is preferred. Morel and Larcheveque (1974) claimed exponential growth up to separations of 1000 km while Lacorata *et al.* (2004) suggest it ceases above 100 km. The dispersion (Fig. 2) indicates exponential growth up to 1000 km, but the growth in the 200–1000 km range is difficult to distinguish from the PDFs. Thus we cannot rule out either the Morel and Larcheveque (1974) or Lacorata *et al.* (2004) scenarios.

b. SCULP

Next we consider pairs from the roughly 700 surface drifters launched during the SCULP program in the Gulf of Mexico (Ohlmann and Niiler, 2005). Most of the drifters were not launched in pairs in this experiment, so LaCasce and Ohlmann (2003) extracted a set of 140 chance pairs, with $r_0 \leq 1$ km. Here we examine a larger set of 188 pairs with $r_0 \leq 2$ km; we use the larger set as it yields somewhat cleaner PDFs. As noted by LaCasce and Ohlmann (2003), the dispersion in the SCULP set is isotropic up to separations of several hundred kilometers.

The dispersion for the 2-km pairs is shown in Figure 5. Also shown are the exponential and cubic curves obtained by least squares fits during the first 5 days. The exponential has

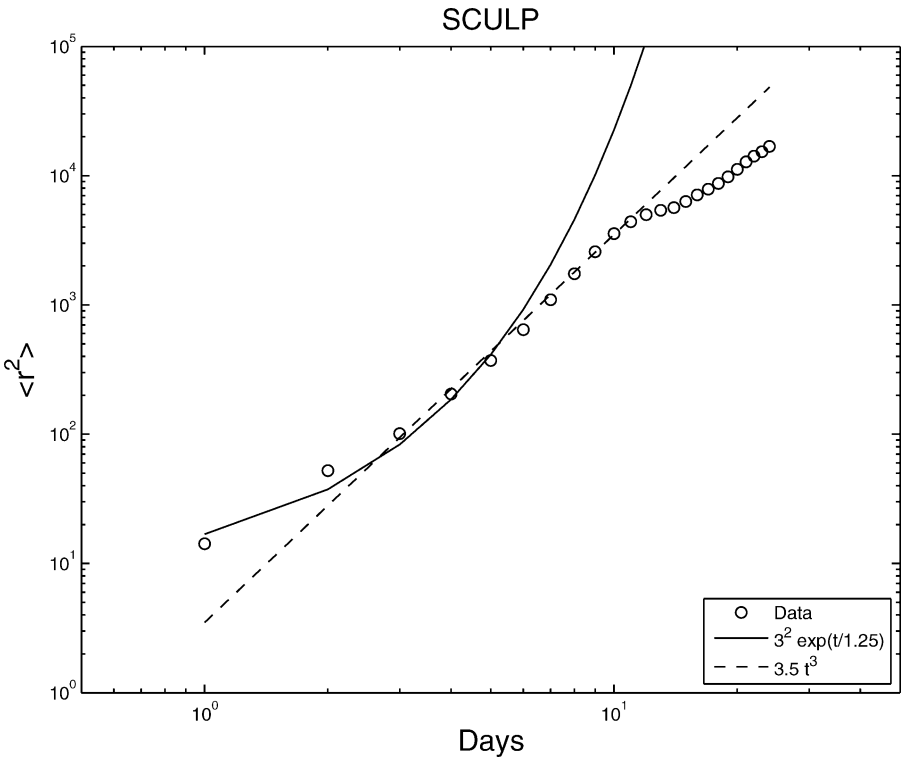

Figure 5. The relative dispersion for the SCULP drifters from the Gulf of Mexico, with the best-fit exponential and cubic curves. The data has a temporal spacing of one day.

$r_0 = 3$ km and an e-folding time of 1.25 days ($T = 10$ days); these values are comparable to those obtained by LaCasce and Ohlmann (2003) for the $r_0 = 1$ km pairs ($r_0 = 3$ km and an e-folding time of 1.8 days). The cubic has an amplitude of 3.5, which corresponds to $\beta = 0.87\,\mathrm{km}^{2/3}/\mathrm{day}$. The dispersion is similar to the exponential during the first few days, but the cubic yields a better fit from days 3–11. Thus Richardson dispersion appears more likely, based on the second moment alone.

The PDFs are compared in Figure 6. At $t = 1$ day, the observed PDF is noisy, but lies somewhat closer to the Lundgren PDF. It has more small separations than the latter, because the initial condition for the Lundgren is a delta function at $r_0 = 3$ km. However, at 5 days the PDF is fairly similar to the Lundgren PDF. At the same time, it exhibits significantly more small separations than the Richardson. This similarity persists at day 10. At 20 days, the PDF is well above the Lundgren curve. However, it is near the Richardson curve at scales above 50 km.

Thus the PDFs suggest exponential growth at small scales. Note too that unlike with the EOLE data, we obtain reasonable agreement with the Lundgren PDF using the value of

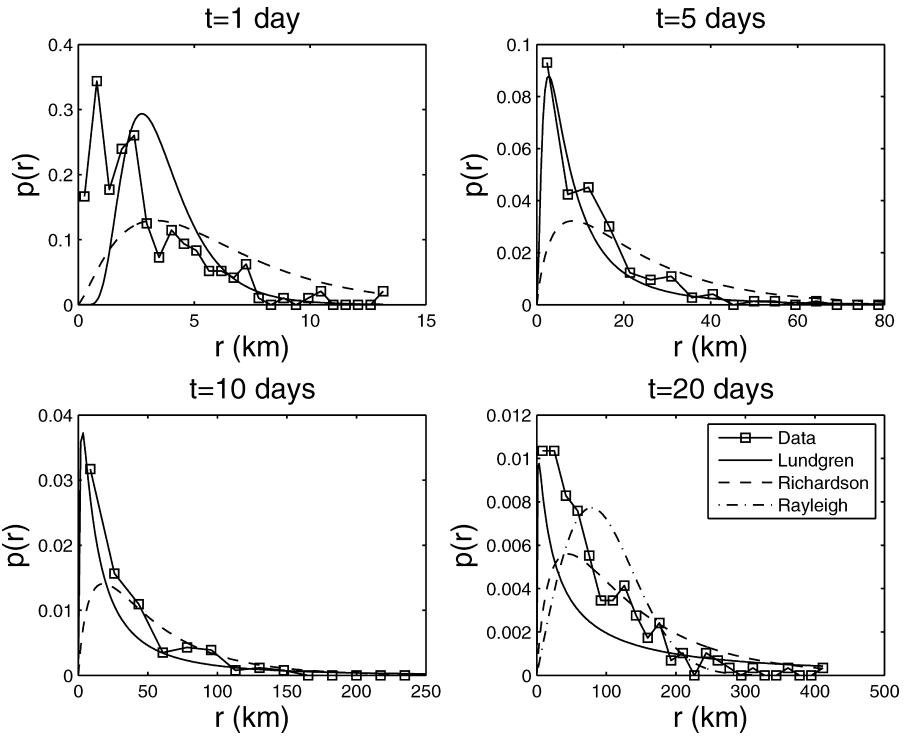

Figure 6. The displacement PDFs for the SCULP data. The Lundgren PDF has $T = 10$ days and $r_0 = 3$ km, and the Richardson PDF has $\beta = 0.87\,\mathrm{km}^{2/3}/\mathrm{day}$ and the same value of r_0.

r_0 obtained from fitting the dispersion. However, as with the EOLE data, it is difficult to determine over what range exponential growth is occurring. The upper limit could be the deformation radius, which is approximately 50 km, as suggested by LaCasce and Ohlmann (2003). But it is also possible the upper range is 10 km; at larger scales the PDF is often between the Lundgren and Richardson PDFs. The proximity of the latter and the noise in the observed PDF at the larger scales make it difficult to say which is preferred.

Note too the SCULP PDFs are not close to the Rayleigh distribution at the end. Neither do we see a final period of linear growth in the relative dispersion. The super-diffusive spreading persists to the largest sampled scales, as noted by LaCasce and Ohlmann (2003).

c. POLEWARD

In the POLEWARD experiment, 150 surface drifters were launched in the Nordic Seas over a period spanning 2007–2009 (Koszalka *et al.*, 2009). The drifters were deployed in pairs and triplets, yielding a number of original pairs. Here we examine the same set of 93 pairs studied by Koszalka *et al.* (2009), with $r_0 \leq 2$ km. Of these, 67 were original pairs.

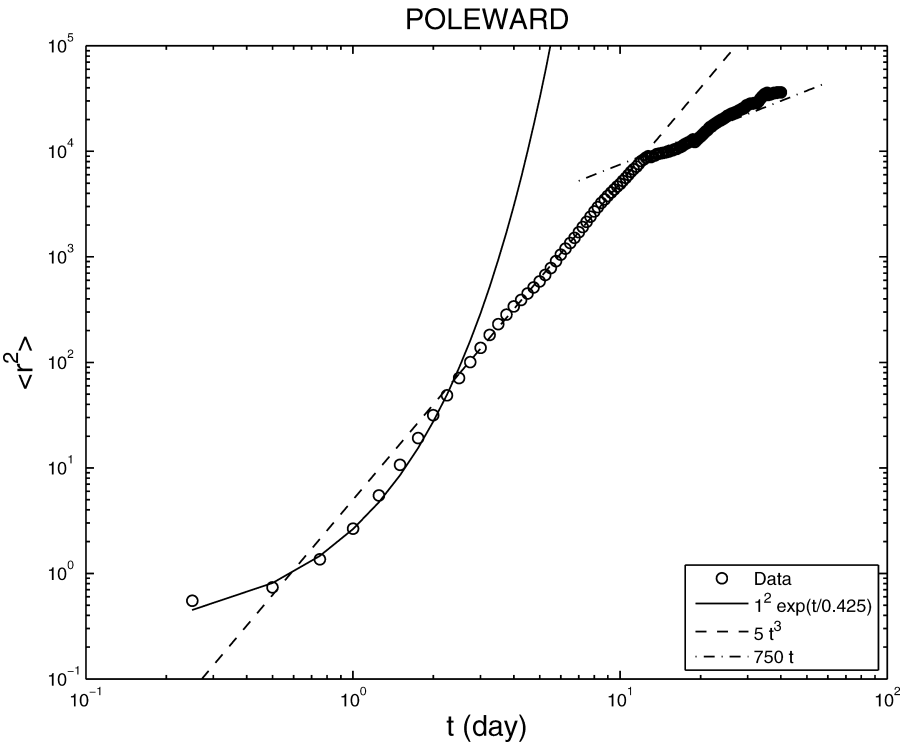

Figure 7. The relative dispersion for the POLEWARD drifter set in the Nordic Seas with best-fit exponential and cubic curves. The temporal resolution is 1/4 of a day.

Koszalka *et al.* (2009) found that the dispersion below the deformation radius, 10 km, was exponential with an e-folding time of about a half day. The dispersion between 10–100 km was better fit with a cubic while that at separations larger than 100 km increased linearly in time. The dispersion was isotropic below 100 km and meridionally anisotropic at larger scales, the latter reflecting advection by the Norwegian Atlantic Current which is similarly oriented in the region. They interpreted the intermediate range as resulting from an inverse energy cascade, having ruled out dispersion by the mean shear.

The dispersion is shown in Figure 7. The dispersion during the first 2.5 days is well fit by an exponential with an initial separation $r_0 = 1$ km and an e-folding time of 0.425 days ($T = 3.4$ days). The best-fit cubic is close to the observed dispersion between days 3 and 10. The amplitude, 5, corresponds to $\beta = 0.98\,\mathrm{km}^{2/3}/\mathrm{day}$. After day 12, the dispersion increases roughly linearly in time.

The PDFs are shown in Figure 8. As with the SCULP data, the observed PDF at 1 day is noisy and different from the two theoretical curves. But by 3 days, the PDF is quite close to the Lundgren distribution below 10 km. The result is similar at 5 days, although the observed PDF is noisy at the larger separations. It is noisier still at 15 days but is near both

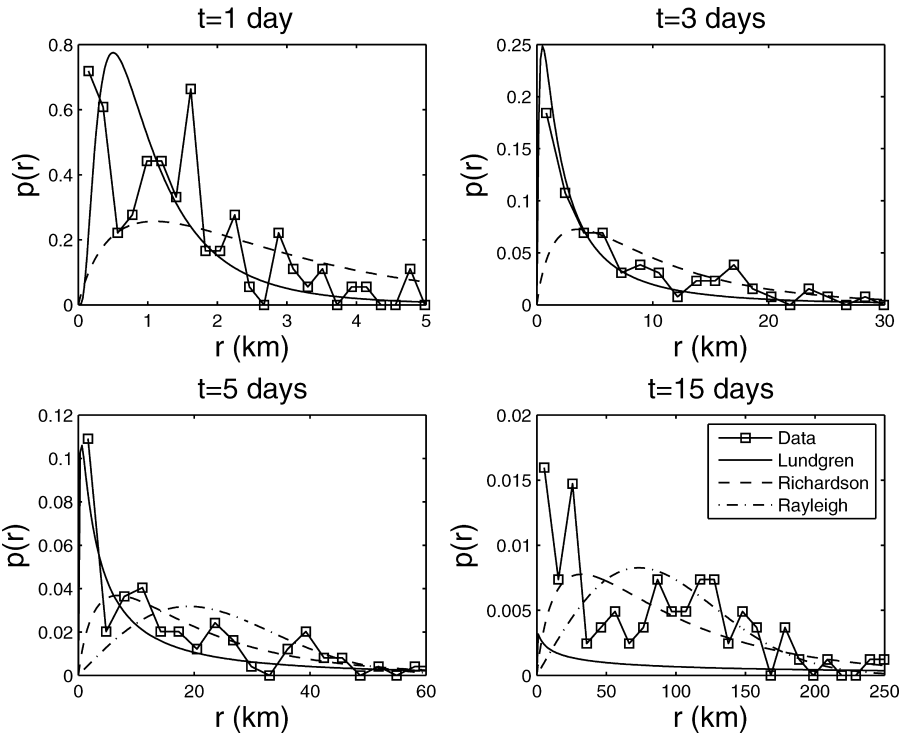

Figure 8. The displacement PDFs for the POLEWARD data. The Lundgren PDF has $T = 3.4$ days and $r_0 = 1$ km, and the Richardson PDF has $\beta = 0.98\,\mathrm{km}^{2/3}/\mathrm{day}$ and the same value of r_0.

the Richardson and Rayleigh curves, except at small separations. Koszalka *et al.* (2009) showed that the PDF at day 40 clearly resembles the Rayleigh distribution.

Thus these results support the conclusions of Koszalka *et al.* (2009). The similarity to the Lundgren distribution at small scales supports exponential growth. However, it is not possible to distinguish the behavior at the intermediate scales, from 10–100 km, using the PDFs. This again is due to the uncertainty at these separations. Getting a better result presumably requires more pairs.

4. Turbulence simulation

A large number of pairs is possible of course with a numerical simulation. In the preceding examples, we saw evidence of exponential growth below the deformation radius. But it was difficult to discern the dispersion at larger scales. If energy is being injected at or near the deformation radius, we would expect to see an enstrophy cascade to smaller scales and an energy cascade to larger (Salmon, 1980). Here we examine separation PDFs for such a case, using a 2-D turbulence simulation forced at intermediate scales. With this we can have a larger number of pairs, perhaps permitting us to capture the Richardson dispersion at intermediate scales.

As noted, Boffetta and Sokolov (2002) compared separation PDFs to the asymptotic Richardson distribution using particles in simulated 3-D turbulence and LaCasce (2010) tested the Lundgren distribution in simulations of a 2-D enstrophy cascade. But none have examined the evolving PDFs with the forcing at intermediate scales, in which both cascades are occurring simultaneously.

For the simulation, we used the numerical code used by (Flierl *et al.*, 1987; LaCasce and Brink, 2000; LaCasce, 2008b, 2010). The code solves the barotropic vorticity equation, given by:

$$\frac{\partial}{\partial t}\zeta + J(\psi, \zeta) = \mathcal{F} - \mathcal{D} \tag{22}$$

where ψ is the velocity streamfunction, $\zeta = \nabla^2\psi$ the relative vorticity, $J(,)$ the Jacobian function and $\mathcal{F}$ and $\mathcal{D}$ are the applied forcing and dissipation. The domain is doubly-periodic, with 512^2 grid points.

The forcing was isotropic and applied in the wavenumber range $\kappa = [30, 35]$, with random phases in space and time. The forcing amplitude was adjusted to yield a final (dimensionless) kinetic energy of around 1.0. We used linear (Rayleigh) dissipation,

$$\mathcal{D} = -R\zeta \tag{23}$$

with $R = 0.1$. The model also has an exponential cut-off filter which removes enstrophy at the smallest scales (LaCasce, 1996).

The time-average spectrum from the simulation is shown in Figure 9. The enstrophy cascade extends from the forcing range to roughly wavenumber 200, where the filter is acting. The enstrophy flux in this range (not shown) is positive (downscale) and approximately constant. Nevertheless, the spectral slope is roughly -4 and thus greater than the theoretical value of -3. This is due to the Rayleigh damping; simulations with damping acting only at larger scales yield slopes closer to -3 (LaCasce, 2010). Nevertheless, because the slope is greater than -3, one still expects exponential growth for pair separations. The slope in the energy cascade range is near $\kappa^{-5/3}$, albeit over slightly less than a decade of wavenumbers.

Once the model reached a statistical steady state, we deployed 2000 particles on a uniform grid and advected them with a fourth-order interpolation scheme. The initial particle separation was $r_0 = 0.01$, which is comparable to the model grid size. Note the forcing range corresponds to separations of $r = [0.25, 0.3]$.

The dispersion is shown in Figure 10. The curve is very similar to that in Figure 7 for the POLEWARD drifters. The initial period is well-fit with an exponential, with an e-folding time of 0.55 and an initial separation of 0.009. The intermediate range can be fit with a cubic, with an amplitude of 0.2. The latter implies an energy dissipation rate which is comparable to that observed for the run. The dispersion in the late period can be fit with a linear function with an amplitude of 2.0.

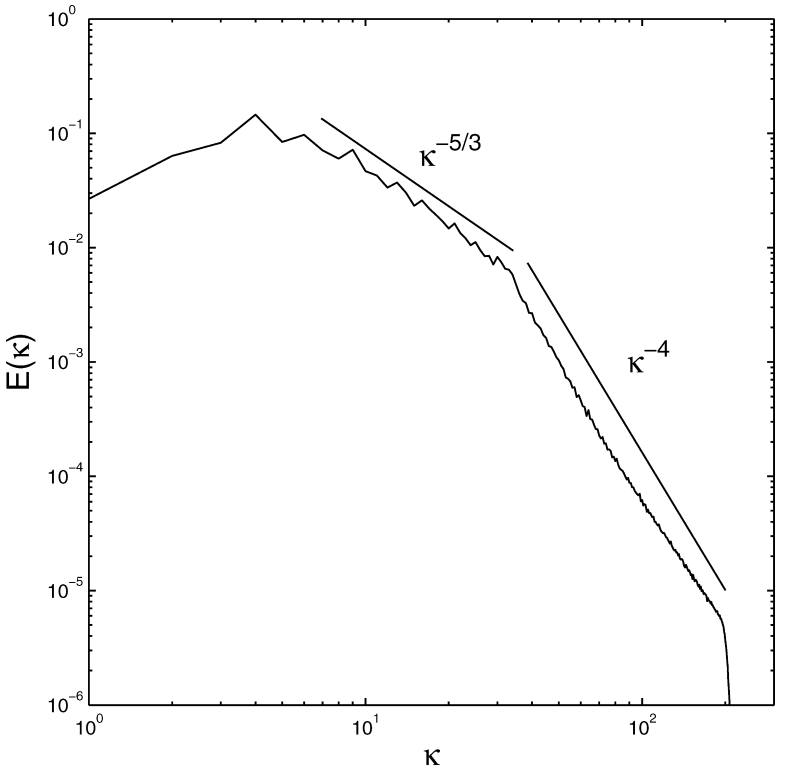

Figure 9. The kinetic energy spectrum for a 2-D turbulence simulation forced in the wavenumber range $\kappa = [35, 40]$.

The PDFs from the data are compared with the (full) Richardson and Lundgren distributions in Figure 11. At an early time, $t = 0.2$, the particle PDF resembles the Lundgren PDF. Note in this case, the actual initial distribution *is* also essentially a delta-function. At $t = 0.4$, the observed and Lundgren PDFs are very similar over the range of scales below the forcing scale of $r \approx 0.3$. At $t = 1$, the PDF still resembles the Lundgren PDF below the forcing range, but also indicates more small separations. At separations greater than about 0.4, the PDF is closer to the Richardson curve. At $t = 2$, the PDF is closest to the Richardson curve, except at the smallest separations. At the largest separations, i.e. $r > 1.5$, the PDF appears to shift toward the Rayleigh distribution. The dispersion (Fig. 10) also shifts to linear growth between $r = 1$ and $r = \sqrt{10}$, which is consistent.

Thus there are several similarities with the *in situ* cases. The PDFs clearly resemble the Lundgren PDF at small scales, and at later times there are more small separations than indicated by the Lundgren solution. As time progresses, the Lundgren curve falls below the observed PDF, because the growth at scales exceeding the deformation radius is slower than exponential.

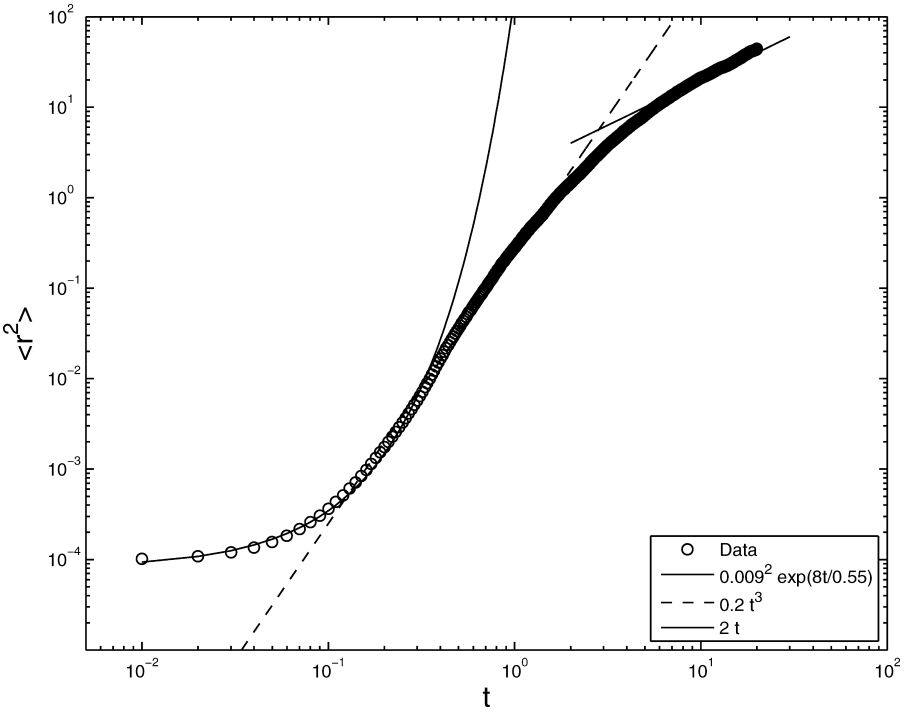

Figure 10. The relative dispersion in the turbulence simulation, for 2000 particles. Also shown is a best-fit exponential, a cubic and a linear function.

However, the difference here is that there is a better indication of Richardson growth at intermediate scales. We see a clear shift toward the Richardson PDF, particularly at the later times. Thus while there are many similarities with the in situ data sets, particularly the POLEWARD set, the transitions are more clearly observed here. This is because there are more pairs: five times the number of particles as in the EOLE set and twenty times the number in POLEWARD.

5. Summary and discussion

We have examined PDFs of particle pair separations from *in situ* data and from a turbulence simulation. We compared these PDFs with three analytical solutions which derive from a Fokker-Planck equation describing the evolution of the separation PDFs. One solution is the Rayleigh distribution, which applies for uncorrelated pair motion. The other two are for the inertial ranges in 2-D turbulence. One, for the enstrophy cascade, is due to Lundgren (1981). The other is a new solution, for the energy cascade. This asymptotes to the 2-D analogue of Richardson's (1926) solution.

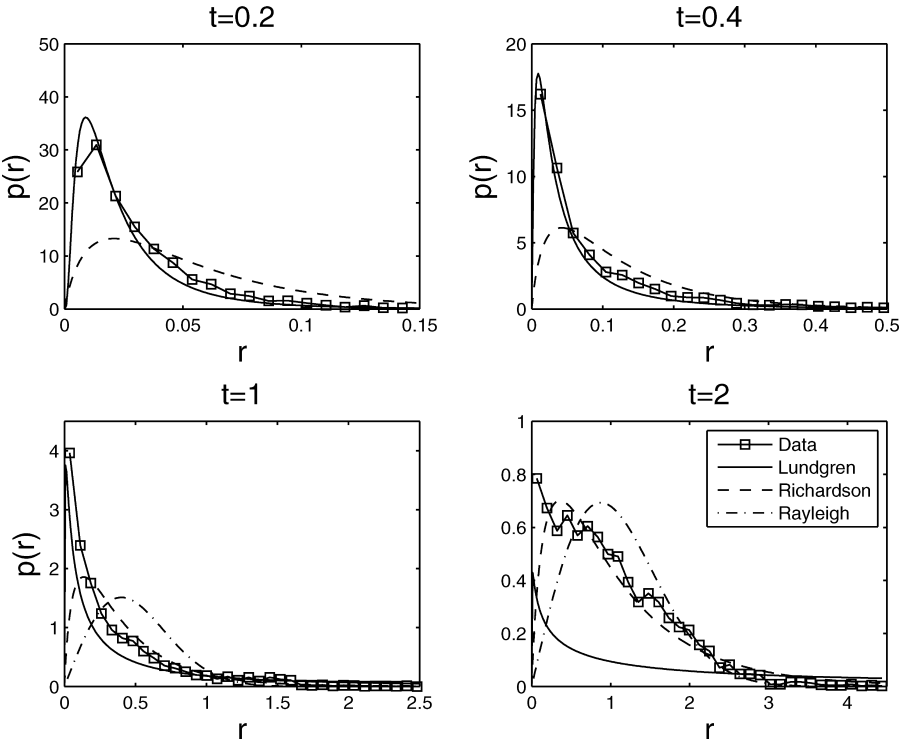

Figure 11. The separation PDFs for the turbulence simulation. Also shown are the Lundgren PDFs (solid), Richardson PDFs (dashed) and Rayleigh PDFs (dash-dot) using parameters derived from the fits shown in Figure 10.

The turbulence simulation was for a 2-D fluid forced randomly in a wavenumber band at intermediate scales. So there was an enstrophy cascade below the forcing scale and an energy cascade above. Consistent with expectations (e.g. Bennett, 1984; Babiano *et al.*, 1990), the relative dispersion grew exponentially below the forcing scale and as time cubed above, until the pairs reached the domain scale when the dispersion increased linearly in time. The separation PDFs evolved consistent with the solution of Lundgren (1981) at small scales. At intermediate scales, the PDFs were similar to the Richardson PDF and at large scales, to the Rayleigh distribution.

The results in the three *in situ* data sets were similar at the smallest scales. In particular, the PDFs resemble the Lundgren solution, and differed significantly from the Richardson PDF. The behavior at intermediate scales was harder to discern, due to uncertainty at large separations. Typically though, the PDF lay between the Lundgren and Richardson distributions.

Thus the data sets are consistent in their indication of nonlocal dispersion at small scales, with pair separations growing exponentially in time. The results thus support similar

assertions made by Morel and Larcheveque (1974), Er-el and Peskin (1981), LaCasce and Ohlmann (2003), Ollitrault *et al.* (2005) and Koszalka *et al.* (2009). However, the results are less clear with regards to the range of scales over which exponential growth is occurring. It is possible the exponential growth proceeds to the deformation radius, as suggested by the previous authors. However, the similarity with the Lundgren distribution is clear only at smallest scales.

Nonlocal dispersion implies a wavenumber energy spectrum of κ^{-3} or steeper. Velocity measurements from commercial aircraft in the upper troposphere suggest a κ^{-3} spectrum from the deformation radius down to roughly 500 km; at smaller scales, the spectrum has a $\kappa^{-5/3}$ slope, as in an energy cascade (Nastrom and Gage, 1985). Lacorata *et al.* (2004) suggest that Richardson dispersion is occurring in the 100–1000 km range, consistent with the shallower spectrum. But their results and ours point to a steeper spectrum at scales below 100–200 km. How this can be reconciled with the aircraft spectra is unclear. However, the EOLE and TWERLE measurements are from the lower stratosphere in the Southern Hemisphere while the aircraft measurements were made in the upper troposphere in the Northern Hemisphere; so it's not certain the results need agree. Previous authors have concluded the spectra are steep in the stratosphere (e.g. Shepherd *et al.*, 2000), and this would yield exponential dispersion. Tests of the dispersion in the upper troposphere would be beneficial in this regard.

Eulerian spectral estimates for the ocean are few, and the results at sub-deformation scales are particularly uncertain (Stammer, 1997). LeTraon *et al.* (2008) suggest the spectra are consistent with a $\kappa^{-5/3}$ energy spectrum, albeit with limited resolution of sub-deformation scales. But a recent result, derived from ADCP measurements from the merchant vessel *Oleander* in the Gulf Stream region, indicates a κ^{-3} spectrum for both kinetic and potential energy below roughly 100 km (Wang *et al.*, 2010). The present results are thus consistent, at least at small scales. However, our data come from the Gulf of Mexico and the Nordic Seas. The existing relative dispersion studies in the Gulf Stream region instead favor Richardson dispersion (LaCasce and Bower, 2000; Ollitrault *et al.*, 2005; Lumpkin and Ellipot, 2010). So the Gulf Stream region also deserves further attention.

The PDFs are generally more effective at gauging the dispersion at small scales than at larger ones. The reason is that the small separations are more frequent, while the larger separations correspond to "extreme events." Thus the wings of the PDF are noisier, complicating the identification of the dispersion regime. The best is to have more pairs. Then the behavior is clearer, as in the turbulence simulation considered here.

PDFs are also useful in quantifying dispersion when the latter itself is equivocal. The initial dispersion in the SCULP set is arguably a better fit with a cubic than an exponential, but the PDFs are closer to the Lundgren distribution. Since the PDFs are non-Gaussian, the dispersion can be a misleading indication of the behavior. Thus it is desirable to use higher order moments, or the PDF, in addition to dispersion.

An important issue for experiments is the initial pair separation, which is limited by the spatial resolution of the instruments. The resolution of 1 km in the POLEWARD experiment

permitted only one decade of sampled scales below the deformation radius of 10 km. If exponential growth is occurring below the deformation radius, then sampling the dispersion over n e-folding time scales requires that the initial separation be $r_0 = L_d/\exp(n/2)$. Having an initial spacing one tenth the deformation radius corresponding to 4.6 e-folding times, a relatively short period.

Another issue for experiments concerns chance and original pairs. Previous studies found no significant differences when using either one (Morel and Larcheveque, 1974; Er-el and Peskin, 1981; LaCasce, 2008a; Koszalka *et al.*, 2009). However, Haza *et al.* (2008) found a difference in simulations of trajectories in the Adriatic, due to inhomogeneities in the flow. The EOLE results (Sec. 3a) indicate that the chance pairs have a longer initial adjustment prior to the exponential growth phase. This may occur because chance pairs have initial positions which are correlated with their velocities (e.g. Babiano *et al.*, 1990). Thus at the early times, the chance pair dispersion was greater than that for the original pairs, and the fits to the Lundgren PDF indicated an initial separation for the chance pairs which was twice that for the original pairs. The results for the POLEWARD set were the clearest of the three examined here, and over 2/3 of those pairs were original. So the present results suggest original pairs are superior for characterizing relative dispersion. This argues in favor of deploying drifters or floats in pairs or clusters in experiments.

In all the cases examined here, the separation PDFs were non-Gaussian. This has been noted previously (Er-el and Peskin, 1981; Davis, 1985; LaCasce and Bower, 2000; LaCasce and Ohlmann, 2003; Ollitrault *et al.*, 2005). Batchelor (1952) proposed an F-P equation with a Gaussian solution under an energy cascade, and Sullivan (1971) found support for this with dye measurements at the surface of Lake Huron. But the present results do not support this; so long as the pair velocities were correlated in our examples, the PDFs were non-Gaussian. Indeed, we observe that the non-Gaussian PDFs persist even *after* the pair velocities cease to be correlated, indicating a "memory" of the initial dispersion.

Acknowledgments. I wasn't a student of George's or even a post-doc, but George was the thesis advisor of my thesis advisor—so I'm part of the family tree. I know George personally through the GFD summer program at WHOI because I often sit beside him in the back row. I know George professionally through his role as editor of JMR and I've always had enormous respect for him in this. Unlike many editors, George really read the submissions. He solicited reviewers' comments, of course, but rather than simply passing those comments back to the author, George assimilated them with his own opinions. This could work both ways. He decided my first article was too long (by half), without sending it for review. But he accepted a later revised article before the reviewers had seen it a second time—and that while picking figs in Australia (according to Doreen Orciari). This personal touch makes JMR an entirely different experience for an author, particularly in these days of electronic submission and "rendering" packages.

The quasi-geostrophic model was provided by Glenn Flierl and the simulations were made on the TITAN cluster at the University of Oslo. The POLEWARD drifter data are archived at NOAA/AOML. The EOLE data were provided by Albert Hertzog (LMD, Paris). Special thanks to Inga Koszalka for further processing both data sets. The SCULP drifter data is courtesy of P. Niiler and C. Ohlmann. I enjoyed several email exchanges with Andrew Bennett, who clarified a number of theoretical points,

and Rick Lumpkin and I discussed the FSLE. Three anonymous reviewers made comments on the first draft which led to several improvements. The work was supported by the Poleward project, funded by the Norwegian Research Council Norklima program (grant number 178559/S30) and the BIAC (Bipolar Atlantic Thermohaline Circulation) project, funded by the Norwegian Research Council under the International Polar Year.

REFERENCES

Artale, V., G. Boffetta, A. Celani, M. Cencini, and A. Vulpiani. 1997. Dispersion of passive tracers in closed basins: Beyond the diffusion coefficient. Phys. Fluids, *9*, 3162–3171.

Aurell, E., G. Boffetta, A. Crisianti, G. Paladin, and A. Vulpiani. 1997. Predictability in the large: An extension of the concept of lyapunov exponent. J. Phys. A: Math. Gen., *30*, 1–26.

Babiano, A., C. Basdevant, P. LeRoy, and R. Sadourny. 1990. Relative dispersion in two-dimensional turbulence. J. Fluid Mech., *214*, 535–557.

Batchelor, G. K. 1950. The application of the similarity theory of turbulence to atmospheric diffusion. Quart. J. Roy. Meteor. Soc., *76*, 133–146.

—— 1952. Diffusion in a field of homogeneous turbulence II: The relative motion of particles. Proc. Cambridge Phil. Soc., *48*, 345–362.

Bennett, A. 1984. Relative dispersion: local and nonlocal dynamics. J. Atmos. Sci., *41*, 1881–1886.

—— 2006. Lagrangian fluid dynamics, Cambridge University Press, Cambridge, 286 pp.

Boffetta, G. and I. M. Sokolov. 2002. Relative dispersion in fully developed turbulence: The Richardson's law and intermittency corrections. Physica A, *88*, 094501.

Capet, X., P. Klein, B. L. Hua, G. Lapeyre, and J. McWilliams. 2008. Surface kinetic energy transfer in quasi-geostrophic flows. J. Fluid Mech., *604*, 165–174.

Charney, J. G. 1971. Geostrophic turbulence. J. Atmos. Sci., *28*, 1087–1095.

D'Agostino, R. B. and M. A. Stephens. 1986. Goodness-of-fit Techniques, Marcel-Dekker, 576 pp.

Davis, R. E. 1985. Drifter observations of coastal surface currents during CODE: The statistical and dynamical view. J. Geophys. Res., *90*, 4756–4772.

Er-el, J. and R. Peskin. 1981. Relative diffusion of constant-level balloons in the southern hemisphere. J. Atmos. Sci., *38*, 2264–2274.

Flierl, G. R., P. Malanotte-Rizzoli, and N. J. Nabusky. 1987. Nonlinear waves and coherent vortex structures in barotropic β-plane jets. J. Phys. Oceanogr., *17*, 1408–1438.

Haza, A. C., A. C. Poje, T. M. Özgökmen, and P. Martin. 2008. Relative dispersion from a high-resolution coastal model of the adriatic sea. Ocean Modelling, *22*, 48–65.

Held, I. M., R. T. Pierrehumbert, S. T. Garner, and K. L. Swanson. 1995. Surface quasi-geostrophic dynamics. J. Fluid Mech., *282*, 1–20.

Isern-Fontanet, J., G. Lapeyre, P. Klein, B. Chapron, and M. W. Hecht. 2008. Three-dimensional reconstruction of oceanic mesoscale currents from surface information. J. Geophys. Res., *113*, C09005–C09034.

Jullien, M.-C. 2003. Dispersion of passive tracers in the direct enstrophy cascade: Experimental observations. Phys. Fluids, *15*, doi:10.1063/1.1585030.

Jullien, M.-C., J. Paret, and P. Tabeling. 1999. Richardson pair dispersion in two-dimensional turbulence. Phys. Rev. Lett., *82*, 2872–2875.

Koszalka, I., J. H. LaCasce, and K. A. Orvik. 2009. Relative dispersion in the Nordic Seas. J. Mar. Res., *67*, 411–433.

Kraichnan, R. H. 1966. Dispersion of particle pairs in homogeneous turbulence. Phys. Fluids, *9*, 1937–1943.

—— 1967. Inertial ranges in two-dimensional turbulence. Phys. Fluids, *10*, 1417–1423.

LaCasce, J. H. 2000. Floats and f/h. J. Mar. Res., *58*, 61–95.
—— 2008a. Statistics from Lagrangian observations. Progr. Oceanogr., *77*, 1–29.
—— 2008b. The vortex merger rate in freely-decaying, 2-D turbulence. Phys. Fluids, *20*, 085102.
—— 2010. Pair separtions in the 2-D turbulent enstrophy range. Phys. Fluids (in prep).
—— 1996. Baroclenic Vortices over a slopping bottom, PhD thesis, MIT/WHOI.
LaCasce, J. H. and A. Bower. 2000. Relative dispersion at the surface in the subsurface North Atlantic. J. Mar. Res., *58*, 863–894.
LaCasce, J. H. and K. Brink. 2000. Geostrophic turbulence over a slope. J. Phys. Oceanogr., *30*, 1305–1324.
LaCasce, J. H. and A. Mahadevan. 2006. Estimating subsurface horizontal and vertical velocities from sea-surface temperature. J. Mar. Res., *64*, 695–721.
LaCasce, J. H. and C. Ohlmann. 2003. Relative dispersion at the surface of the Gulf of Mexico. J. Mar. Res., *61*, 285–312.
Lacorata, G., E. Aurell, B. Legras, and A. Vulpiani. 2004. Evidence for a $\kappa^{-5/3}$ spectrum from the eole lagrangian balloons in the low stratosphere. J. Atmos. Sci., *61*, 2936–2942.
Lapeyre, G. and P. Klein. 2006. Dynamics of upper oceanic layers in terms of surface quasigeostrophy theory. J. Phys. Oceanogr., *36*, 165–176.
LeTraon, P. Y., P. Klein, B. L. Hua, and G. Dibarboure. 2008. Do altimeter wavenumber spectra agree with interior or surface quasigeostrophic theory? J. Phys. Oceanogr., *38*, 1137–1142.
Lin, J.-T. 1972. Relative dispersion in the enstrophy-cascading inertial range of homogeneous two-dimensional turbulence. J. Atmos. Sci., *29*, 394–395.
Lumpkin, R. and S. Ellipot. 2010. Surface drifter pair spreading in the North Atlantic. J. Geophys. Res., (in press).
Lundgren, T. S. 1981. Turbulent pair dispersion and scalar diffusion. J. Fluid Mech., *111*, 27–57.
Morel, P. and W. Bandeen. 1973. The eole experiment, early results and current objectives. Bull. Am. Met. Soc., *54*, 298–306.
Morel, P. and M. Larcheveque. 1974. Relative dispersion of constant-level balloons in the 200 mb general circulation. J. Atmos. Sci., *31*, 2189–2196.
Nastrom, G. D. and K. S. Gage. 1985. A climatology of atmospheric wavenumber spectra of wind and temperature observed by commerical aircraft. J. Atmos. Sci., *42*, 959–960.
Ohlmann, J. C. and P. P. Niiler. 2005. A two-dimensional response to a tropical storm on the Gulf of Mexico shelf. Progr. Oceanogr., *29*, 87–99.
Ollitrault, M., C. Gabillet, and A. C. de Verdiere. 2005. Open ocean regimes of relative dispersion. J. Fluid Mech., *533*, 381–407.
Ott, S. and J. Mann. 2000. An experimental investigation of the relative diffusion of particle pairs in three-dimensional turbulent flow. J. Fluid Mech., *422*, 207–233.
Press, W. H., S. A. Teukolshy, W. T. Vetterling, and B. P. Flannery. 1992. Numerical Recipes in FORTRAN: The art of scientific computing, Cambridge University Press, Cambridge, 963 pp.
Richardson, L. F. 1926. Atmospheric diffusion on a distance-neighbour graph. Proc. R. Soc. Lond. A, *110*, 709–737.
Salazar, J. P. L. C. and L. R. Collins. 2009. Two particle dispersion in isotropic turbulent flows. Annu. Rev. Fluid Mech., *41*, 405–432.
Salmon, R. 1980. Baroclinic instability and geostrophic turbulence. Geophys. Astrophys. Fluid Dyn., *15*, 167–211.
Shepherd, T. G., J. N. Koshyk, and K. Ngan. 2000. On the nature of large-scale mixing in the stratosphere and mesosphere. J. Geophys. Res., *105*, 12,433–12,446.
Stammer, D. 1997. Global characteristics of ocean variability estimated from regional topex/poseidon altimeter measurements. J. Phys. Oceanogr., *47*, 1743–1769.

Sullivan, P. J. 1971. Some data on the distance-neighbour function for relative diffusion. J. Fluid Mech., *47*, 601–607.

Taylor, G. I. 1921. Diffusion by continuous movements. Proc. Lond. Math. Soc., *20*, 196–212.

Tulloch, R. and K. Smith. 2006. A theory for the atmospheric energy spectrum: Depth-limited temperature anomalies at the tropopause. Proc. Nat. Acad. Sci., *103*, 14960–14694.

—— 2009. Quasigeostrophic turbulence with explicit surface dynamics: Application to the atmospheric energy spectrum. J. Atmos. Sci., *66*, 450–467.

Wang, D.-P., C. N. Flagg, K. Donohue, and H. T. Rossby. 2010. Wavenumber spectrum in the Gulf Stream from shipboard ADCP observations and comparison with altimetry measurements. J. Phys. Oceanogr., *40*, 840–844.

Received: *3 March, 2010*; revised: *25 October, 2010*.